

# On the Sensitivity of Deflagrations in Chandrasekhar Mass White Dwarf to Initial Conditions

Eli Livne<sup>1</sup>, Shimon M. Asida<sup>1</sup>, Peter Höflich<sup>2</sup>

Received \_\_\_\_\_; accepted \_\_\_\_\_

Submitted to Ap.J.

---

<sup>1</sup>Racah Institute of Physics, The Hebrew University, Jerusalem, Israel

<sup>2</sup>Department of Astronomy, The University of Texas, Austin, UT 85721

## ABSTRACT

We analyze the sensitivity of the flame propagation in a Chandrasekhar mass white dwarf to initial conditions during the subsonic burning phase (deflagration), using 2D simulations of the full WD. Results are presented for a wide variety of initial flame distributions including central and off-center single point and multi-point, simultaneous and non-simultaneous, ignitions. We also examine the effects of convective velocity field which should exist at the core before the thermo-nuclear runaway.

Our main conclusion suggests that the amounts of burning products and their distributions through the deflagration phase are extremely sensitive to initial conditions, much more sensitive than presented in previous studies. In particular, we find that more complex configurations such as even slight off-center ignitions, non-simultaneous multi-point ignitions and velocity fields tend to favor solutions in which individual plumes rise faster than the bulk of a typical Rayleigh-Taylor driven, unstable burning front. The difference to previous calculations for an octant of a WD may be understood as a consequence of the suppression of  $l=1,2$  modes. Our results are consistent with full star calculations by the Chicago group. Moreover, the total amount of nuclear burning during the phase of subsonic burning depends sensitively on the initial conditions and may cause the WD to pulsate or to become unbound. We discuss the implications of the results on current models for Type Ia SNe, limitations imposed by the 2-D nature of our study, and suggest directions for further study.

*Subject headings:* supernovae, hydrodynamics

## 1. Introduction

The last decade has witnessed an explosive growth of high-quality data for thermonuclear explosions of a White Dwarf Star (WD), the Type Ia Supernovae (SNe Ia). Advances in computational methods provide new insights into the physics of the phenomenon and a direct, quantitative link between observables and explosion physics. Both trends combined provided spectacular results, allowed to address, to identify specific problems and to narrow down the range of scenarios. However, with the advances came the realization that observational constraints seem to be at odds with the most elaborated calculations for deflagration fronts, one of the central parts in the currently most favored model, the thermonuclear explosion a Chandrasekhar mass WD.

The  $M_{Ch}$  scenario requires an initial phase of pre-expansion because, otherwise, almost the entire WD would burn to  $^{56}Ni$ , in contradiction to the observation which show a significant amount of intermediate mass elements, namely O, Si, and S. This pre-expansion is commonly believed to occur during an initial phase of a slow deflagration that preserves the WD structure but decreases the binding energy. In absence of strong mixing, the pre-expansion depends mainly on the total amount of burning but hardly on its actual rate Dominguez & Höflich(2000). Successful spherical models need either a rapidly increasing deflagration speed and no radial mixing (similar to W7 Nomoto *et al.* 1984 – see footnote <sup>2</sup>), or a deflagration-detonation transition (DDT). For 'successful' models,  $\approx 0.2\text{-}0.3 M_{\odot}$  are burned during the deflagration phase leading to a loosely but still bound WD ( $E_{WD,pot} \approx 1\text{--}2 \times 10^{50} erg$ )

---

<sup>2</sup>The pure deflagration model W7 is a spherical model and, consequently, shows a layered structure which is typical for detonations. Realistic 3-D deflagration models do not show a radial layering of the abundances.

The hydrodynamical evolution of a WD undergoing burning by subsonic narrow flame is governed by Rayleigh-Taylor (RT) instability and the consequent buoyancy of hot plumes of ashes. This buoyant motion has two major effects - first, it increases the front surface and therefore enhances the effective burning rate. At the same time the spherical distribution of different elements is being destroyed and a complex structure, 3D by nature, is formed. Therefore, multidimensional simulations became essential for establishing a viable reactive hydrodynamical model for the deflagration phase. Recently, significant progress has been made toward the understanding of the flame physics of deflagrations. Starting from static WD, hydrodynamic calculations of the deflagration fronts have been performed in 2-D (Livne 1993L, Niemeyer & Hillebrandt 1995, Reinecke *et al.* 1999, Lisewski *et al.* 2000) and 3-D (.e.g. Khokhlov 1995, Khokhlov 2001, Reinecke, Hillebrandt & Niemeyer 2002, Gamezo *et al.* 2003, Gamezo *et al.* 2004). As a common result, RT instabilities govern the morphology of the burning front in the regime of linear instabilities, i.e. as long as perturbations remain small. An initially spherical flame propagates outward with a laminar velocity of about 100 km/sec, becomes distorted by Rayleigh-Taylor instabilities, and forms multiple plumes at different scales. Hot, burned matter plumes rise outward due to buoyancy, and cold, unburned matter is pulled toward the inner region. Nuclear burning is ongoing and, as a result, the plumes mainly consists of iron-group elements with a skin of intermediate mass elements produced when the plume reaches low density regions. Overall, the effective burning speed is typically less than 10 % of the sound speed. The energy release by plumes will result in the expansion of the entire envelope and, eventually, the Ni-plumes will 'freeze' out in the expanding envelope. Outer layers of the envelope expand close to the speed of sound and cannot be reached by the burning front. In pure 3D-deflagration models, typically 1/2 to 2/3 of the total mass undergoes nuclear burning and releases about 1. to  $1.3 \cdot 10^{51}$  erg of nuclear energy, and the WD becomes unbound, and produces a 'healthy explosion'. All multi-dimensional, pure deflagration SN models seem to

show the same properties, namely a thick layer of unburned C/O rich matter, a non-radially stratified structure of the burning products, and explosion energies about half of that is required to fit spectra and LCs.

The three dimensional nature is starting to become accessible by direct observations of remnants (Fesen 2004), spectro-polarimetry (Howell *et al.* 2001, Wang *et al.* 2003), early time IR-spectra for subluminous SNe Ia, and late-time spectral line profiles (e.g. Bowers *et al.* 1997, Höflich *et al.* 2003). Some 3-D effects seem to be unavoidable for a system originating from a close binary system with mass overflow because of its interaction with the accretion disk and the companion star (Livne *et al.* 1992, Marietta & Burrows 2000). Other possible reasons include instabilities in the burning front, namely during the deflagration phase, off-center detonations or the transitions from deflagration to detonation, and the rapid rotation of the progenitor. We start to see evidence for all these asymmetries with the noticeable exception for the Ni plumes or, more precisely, we do not see these signatures using the various methods, although they should have been seen. For recent reviews see Branch 1999, Höflich 2005.

Assuming the runaway develops to a deflagration front, the sensitivity of the burning history to initial conditions was first revealed by Niemeyer *et al.* 1996, where a set of several initial ignition configurations have been used for 2D simulations. However, the set was very limited and left open many questions. In general, the authors found that the buildup time of RT-instabilities is shorter corresponding to the larger gravitational acceleration, producing an off-center distributions of iron-group elements. Still the basic characteristics of deflagration burning remain unaltered, namely the chemical distribution and the typical amount of burning. However, one case was unique. In case of an ignition in a single point at 200 km off-center, an isolated hot bubble rises very quickly to the surface, leaving a bound star. Recently, based on 3D calculations, Calder *et al.* (2003) found similar behavior when

ignition occurs only 12 km off-center in an spherical bubble of 50 km in radius. We shall refer to this phenomena as *the single bubble catastrophe* , as in this case the deflagration ends with a dud explosion. In such a case, only a few percents of the star are burned and a large plume of ashes reaches very early the surface of the WD.

Unfortunately, we do not know what should be proper initial conditions for the deflagration phase. The evolution of the WD toward thermonuclear runaway and the initial position of the flame are hardly known. Höflich and Stein (2002) were the first to perform 2D simulations of the last minutes before the runaway. Those simulations show that ignition occurs at a single point off center, at a radius of 30-50 km. They found that generations of rising plumes create a convective velocity field which, by and large, dominates the initial motion of the individual plumes. As a consequence, the transition from non-explosive to explosive burning, the ignition, occurs most likely when a hot plume is dragged downward and compressed. Based on 3-D calculations prior to the runaway, Woosley & Wunch (2004) suggested that large scale velocity pattern is being established on time scales of several minutes which causes hot plumes to be carried outward and, as a consequence, may favor larger off-center ignitions. It is under discussion, whether this global pattern survives the rapid increase of nuclear burning during the last minutes prior to runaway (Höflich 2005).

In this work, we want to study the range of parameters that span the set of very different combustions, between the *single bubble catastrophe* , and the partially 'healthy' explosion. We therefore investigate the influence of a wide variety of initial conditions using our best numerical tools in a parametric manner. We focus on the properties of the deflagration phase and the observational consequences. We vary the number of ignition points and their distribution in space and time. Furthermore, in part of the simulations we take into account a pre-existing velocity field which should develop during the convective burning stage which precedes the runaway. In particular, a major subject of this study is

to understand the conditions at which single bubbles are formed and escape to the surface. Despite the limitations of 2D simulations to give quantitative results to the problem at hand, we believe that qualitatively our 2D results are valid, and should be used in future similar 3D studies.

## 2. Basic Methods and Tools

We have used the 2D code VULCAN (Livne 1993), with new capabilities listed below, to simulate the deflagration phase in an isentropic Chandrasekhar mass WD. The code is based on cylindrical coordinates and is used for many years to simulate astrophysical flows under the assumption of axial symmetry. Since this is a comparative study which focus on the effects of initial conditions, the details of other numerical and physical components of the simulations are not important, provided the simulations are being performed close enough to the 'realistic' case. For example, the initial composition of the WD has important impact on the final abundances, but for our purposes it has only minor effect on the flow and we impose in all the presented simulations the same C-O ratio, namely 1. The isentropic structure of our initial configurations is a very good approximation to a more realistic structure due to two reasons. Firstly, the entropy has little effect on the pressure in the very degenerate part (close to the center) of the star. Secondly, a large part of the star is convective at the final stages of evolution so that an almost isentropic 'convective core' develops around the center. The equation of state is the standard 'eos' for degenerate electrons + radiation + nuclei gas. Simplified reactions network with approximate binding energy have been used (see below more details).

We use 'nearly' polar grids (but cylindrical coordinates) with varying radial spacing and constant angular spacing. The grid in most of the simulations consists of 150 radial zones (logarithmically spaced) and 150 angular zones. Verification runs with 100 and 200

zones in each direction gave very similar results in which the larger patterns are the same and the total energy production vary by a few percents (see figure 5d). In order to avoid the singularity of the polar grid we generate a special finite element grid inside an inner radius of 100 km, which is connected smoothly to the main polar grid. Contrary to conventional polar grids, our hybrid grid enables us to follow transversal motions through the center with little numerical expenses. The only price we pay here is that the spurious numerical errors of the hydrostatic equilibrium are a bit larger in this inner zone. We have tested hydrostatic equilibrium by running the code without burning and found no significant expansion or contraction after a whole one second. Some spurious velocities are seen in the inner zone, where the grid is not polar, but even there those velocities are much smaller than velocities generated by the deflagration.

Several sets of initial conditions, ignition points, were used in order to study the wide range of the unknown ignition parameters. The first set consists of ignition in a sphere of a given radius. This case is similar to the initial conditions used in Gamezo *et al.* 2004. A second set is based on igniting a single point off center on the axis, at a given distance from the center ( see Plewa *et al.* 2004). In a third set we ignite 30 points distributed in a given volume in time and space. Here we extend similar but simultaneous initial conditions used in Röpke & Hillebrandt 2004 to non-simultaneous multi-point cases. The temporal distribution of the points in the non-simultaneous case is exponential with a time scale of 0.1 sec, as suggested in Woosley *et al.* 2004.

Our ignition method does not introduce any abrupt disturbance to the star (which could happen due to careless initial energy deposition at finite ignition regions). In fact, we start always from zero-volume ignition points or point, from which the burning fronts propagate a short distance with some prescribed initial speed. This speed is fast enough to carry the front away from the ignition points in a reasonable time but slow enough to allow

the star to react to the release of energy. The distance on which this initial speed is used is very small, of the order of several grid cells. Only in the first set of simulations, where we want to ignite a sphere of finite radius, we increase this initial radius to the radius of the initial sphere. From there the fronts propagate according to the basic front algorithm described below.

For each set of ignition points we computed two simulations. In the first one we start from a stationary configuration in hydrostatic equilibrium. In a second simulation we added initially a convective velocity field which mimics the early convection which precedes the runaway. The magnitude of this field is comparable to the laminar speed near the center (see subsection 2.2). The simulations presented here are limited to a finite time due to grid limitations. Our grids follow the global expansion of the star but we can not follow at the moment the high speed rise of small bubbles after they reach the surface of the star. To follow the evolution further an extended grid is required, like in Plewa *et al.* 2004. Nevertheless, the conclusions are valid for the early phase deflagrations and delayed detonation models.

## 2.1. Front Propagation and Burning

A special algorithm for front propagation have been developed. Using a special interface tracking algorithm, we utilize the multi-phase capability of the code to improve the accuracy of our simulations. This algorithm minimizes numerical dissipation in the advection step and at the same time enables to define and to advance the location of the front in a very accurate way. We use a 'Volume of Fluid' (VOF) method (see review in Ruben and Stephane 1999) to locate the interface between fuel and ashes, at any given time, in cells containing two phases. Given the partial volumes of those two phases in a cell, we construct the interface in such a way that it is perpendicular to the gradient of phases

and divide the cell into two parts with the given partial volumes. This algorithm, which is very accurate, is used twice in each time step - in the advection (remapping) step and in the burning step, where the propagation of the front is calculated.

The front propagates perpendicular to itself at a speed which is the maximum between the laminar speed and a turbulent speed based on a sub-grid model. We adopt here the simple RT driven formula for the turbulent speed  $v_t = 0.5\sqrt{Agl}$ , where  $A$  is Atwood's number,  $g$  is the gravitational acceleration and  $l$  is a length comparable to the local mesh size. This recipe was first used in this context by Livne (Livne 1993L) and later was calibrated by A. Khokhlov (Khokhlov 1995) using 3D control simulations. More complicated recipes for turbulent speed, which include Kelvin-Helmholtz instability effects at shear layers (Niemeyer & Hillebrandt 1995), are now under investigation, but that study lies beyond the scope of this work. We may comment that uncertainties in the turbulent speed may change the energy production by at least  $10^{50}$  ergs, while they only weakly affect how the ashes are distributed in the ejecta. Those uncertainties remain because both numerical calibrations (Khokhlov 1995) and terrestrial experiments (Niemeyer & Hillebrandt 1995) were not performed in spherically expanding envelopes.

The binding energy is being released in the volume swept by the front locally. Because we are not interested here in detailed nucleosynthesis, and in order to enable the performance of many simulations, the simulations presented here were calculated with simplified rates, which produce accurate enough 'q-value' (the amount of energy released per gram) at various densities. A control simulation where an alpha network have been used gave similar results. Both the alpha network and the simplified rates take into account photo-dissociation, which is the important back-reaction at high density. Thus, the 'q-value' increases from roughly  $3 \times 10^{17} \text{ erg/g}$  at the center to about  $6 \times 10^{17} \text{ erg/g}$  at the low density regions. This q-value underestimates the alpha network q-value at low densities by a few

percents, so that the buoyancy in the simulations is certainly not overestimated.

## 2.2. Early Convection

It was shown numerically (Höflich & Stein 2002) and theoretically that a convective velocity field evolves before the runaway, with convective speed comparable to the laminar speed of the deflagration in its first stages. Consequently, convective speed of 100 km/sec (with typical Mach number of 0.02 at the center) is expected at runaway. However, 2D simulations of the early convection are not only very expensive but they also do not produce a correct hierarchy of scales. To overcome this, we construct a 2D artificial initial velocity field, imposed on the flow at  $t=0$ . The construction uses multi-mode potential flow which is incompressible in the sens that  $\text{div}(\rho\mathbf{v}) = \mathbf{0}$ . The field is generated by imposing a vorticity source which has zero total circulation and is distributed in a given region of the star (inside the convective core). With no 3D simulations of the pre-runaway phase, we can only guess the amplitudes and wavelengths of the source according to the qualitative 2D fields obtained by Höflich & Stein 2002. We found that indeed those fields do not introduce artificial pressure waves and mimic nicely initial (yet unknown) incompressible convective field (see fig.1). Further details will be reported elsewhere.

EDITOR: PLACE FIGURE 1 HERE.

## 3. 2D Simulations - Results

A few snap shots from simulations with a single point ignition are shown in figure 2. Regardless the location of the ignition point they all end up with a single bubble which reaches the surface at a speed of nearly 5000 km/sec. The bubble accelerates mainly after

about 0.5 second, when it rises into the region having large pressure and gravitational slopes (small pressure scale height). In those cases the deflagration incinerates only a few percents of the fuel and the WD remains bound. The effect of early convection in this case is very small and do not change the evolution. Larger distance between the center and the ignition point leads to smaller amount of burning. In large, our results are in very good agreement with the results shown in Plewa *et al.* 2004.

EDITOR: PLACE FIGURE 2 HERE.

The simulations which start with a burning sphere of radius 30 km show different results (figure 3A). Although they all develop bubbles and spikes under the RT instability no single bubble gain enough speed to overcome the global expansion. The nearly homologous expansion keeps the burning zone confined to the central region and burning proceeds at relatively high density. As a result, the amount of energy released is enough to unbind the star. The fact that the obtained energy in our simulation is too small for healthy SNe Ia can be attributed to the well known difference between 2D and 3D simulations. In this sense our results agree with previous 2D and 3D simulations (see introduction). When initial convection is being introduced into the simulation the outcomes change by small amount energy-wise but a very large asymmetry of bubbles develop after one second (figure 3B). This finding should have important implications concerning observables of such models (see conclusions).

EDITOR: PLACE FIGURE 3 HERE.

Multi points ignition cases yield intermediate results, in between the two extreme cases described above. In all those cases we find large asymmetries and effective burning rates which are significantly smaller than those of the spherical case. The asymmetries, which go

together with reduced burning rates, are larger when non-simultaneous ignition is employed or/and when initial convective velocity field is introduced at  $t=0$ . It is enough that one of these physical components will be present in a simulation to induce large asymmetry at late time. Figure 4 show some snap shots of the bubbles distribution after about 1.2 seconds for multi-point cases. One can see that in some cases a single bubble does float to the surface while at other cases the bubbles remain confined to the inner part of the expanding envelop. The main parameter which distinguish between the two cases is the location of the ignition point which runaway first.

EDITOR: PLACE FIGURE 4 HERE.

Figures 5a-5d summarize the energy production rates for the simulations discussed above. In figure 5a we present the results of the simulation with a single off-center ignition. We can see that the energy production is low and only small differences exist between the different cases. The only exception is the case in which the ignition is relatively close to the center (at a radius of 10 kilometers), where more energy is produced. In the simulations with initial burning sphere, energy production exceeds the binding energy, as can be seen in figure 5b. The existence of initial convective velocity field does not affect significantly the energy production (at least until the time in which the first bubble reaches the surface). In figure 5c we can see that in the case of multi-point ignition, initial convective velocity field reduces the energy production. A non-simultaneous ignition has a greater effect as well. Figure 5d presents the sensitivity of the energy production graph to the resolution of the grid for the simulation with simultaneous multi-point ignition (compare to figure 4A).

EDITOR: PLACE FIGURE 5 HERE.

#### 4. Conclusions

The outcomes of a deflagration process in a Chandrasekhar mass WD are determined primarily by the distribution in space and time of the initial flamelets. Different distributions lead to very different evolutions, from dud events to 'reasonable' explosions. The two extreme cases are the runaway of a single point on one side and the spherical volume ignition on the other side. Both cases are not very likely to happen in nature because of the complicated convective structure of the flow before runaway. The single point case leads always to a dud event in which only a few percents of the star are consumed. Whether or not a *confined detonation* (Plewa *et al.* 2004) follows such an event should be examined in full 3D simulations. In this case however it is assumed that no other point runaway during the first second which follows the ignition of the first point. On the other side of the spectrum spherical volume ignition leads to significant burning which unbind the star. In 2D, the energy released is too small to produce acceptable SN but 3D simulations were shown to release much more energy, on the lower side of healthy explosions. The presence of initial convective velocity field show little effect in this case on the total energy released but induce a large asymmetry on the burning region. We may argue that the volumes initially ignited in published 3D simulations are much too big to be realistic. When the radius of the initial burning sphere is reduced to a few kilometers the behavior of the following deflagration becomes more similar to the case of a single point.

In the case of multi-point ignition two effects play important roles. First, the amount of energy released and the structure of the bubbles are very sensitive to the spatial and temporal distribution of the local runaways. With simultaneous multi-point ignition the amount of energy released drops by twenty percent compared to volume ignition and the star is marginally bound (limited to 2D). When non simultaneous multi-point ignition is used we get another drop of twenty percent in the binding energy released, which makes the

explosion model a dud event. The second effect is the presence of initial convective velocity field, which causes a similar drop in the total burning and similarly harm the explosion. We notice however that those two effects are not additive and their joint effect is similar to the effect of each of them. The reason for the drop in energy release in those cases is that once a single or several bubbles escape with high speed the total effective burning rate drops significantly, because burning on the surface of those bubble occurs at very low density.

At large, we find a very diverse space of possible distributions of burning products, as function of initial conditions. Large asymmetries and large variations in burning energy and products are found. Non-simultaneous multi-point ignitions and velocity fields tend to favor solutions in which individual plumes (dud solutions) rise rather than being dominated the typical Rayleigh-Taylor driven, unstable burning fronts. In case of dud-solutions, our results agree well with those of Calder *et al.* 2003. However, in other 3D simulations, the single bubble catastrophe was not observed. We can suggest qualitative explanation to those differences. Gamezo *et al.* (Gamezo *et al.* 2004) start the simulation with a spherical hot bubble of 30 km radius, which maintains hydrostatic equilibrium. However, since they compute only one octant with reflecting boundary conditions the most important low unstable modes are suppressed. Röpke & Hillebrandt (2004) start their simulation with a large number of simultaneous ignition points, distributed inside a radius of 200 km. This causes prompt expansion which tends to suppress the buoyancy of single plumes. Furthermore, their spatial resolution of  $\delta x = 8$  km may be too coarse to allow the instability to develop. In our 2D simulations the grid size at  $r = 100$  km, which is the radius where the plumes start accelerating, is roughly 2 km.

It is beyond the scope of this work to provide a general overview over the relation between observables, possible DDT and the influence of variations in the progenitor. For this purpose, we would like to refer to recent reviews and articles (Branch 1999, Höflich

*et al.* 2003, Gamezo *et al.* 2004, Höflich 2005). Instead, we want to put specifically our results in the context of explosion models, and to evaluate possible observational consequences. We show that deflagration phases vary widely in their energy production from 'dud' events with nuclear energy productions from  $10^{50} erg$  to healthy explosions, and everything in between. This opens up the possibility that the WD undergoes a phase of one or multiple pulsations, a solution which previously has been excluded (Reinecke, Hillebrandt & Niemeyer 2002). Furthermore, the possibility to trigger a detonation by the Zeldovich mechanism during pulsations (Khokhlov *et al.* 1992, Höflich *et al.* 1995) can no longer be ignored. As mentioned in the introduction, spherical explosion models require a pre-expansion of the WD which requires nuclear burning between  $0.2 - 0.3 M_{\odot}$  before a DDT (or a phase of fast deflagrations) occurs. Based on this, it has been suggested (Höflich *et al.* 2003, Höflich 2005) that the DDT should occur during the expansion phase, which is RT dominated. Based on temperature fluctuations scales it has been argued that 'self-induced' DDT is unlikely in this phase (Niemeyer 1999), and some other ('external') mechanisms have been suggested such as shear flow induced instabilities in the layers between initial WD and accreted matter (Höflich *et al.* 2003, Yoon, Langer, & Scheithauer 2004, Yoon & Langer 2004). However, the results shown here should now re-open that discussion by considering non-radial pulsational modes and large scale circulation that may have time to develop and trigger a detonation.

In summary, the results of this work show larger sensitivity of the deflagration products to initial conditions at runaway than assumed or reported before. Therefore, it is urgent to verify these results in a full star 3D simulations (which are unfortunately beyond the available computer capabilities of the authors). Even if only partially verified (smaller sensitivity in 3D ?) they cast serious questions concerning the currently standard mechanism for SNIa's and call for more work focused on pre-runaway evolution.

We would like to acknowledge discussions with all our colleges. E. Livne thanks P. Mazzali, J. Stein and A. Glasner for fruitful discussions. This work has been supported by the NASA grants (NAG5-7937, HST-GO-10118.05-A) and by NSF grant AST0307312 to PAH.

## REFERENCES

Bowers, E. J. C., Meikle, W. P. S., Geballe, T. R., Walton, N. A., Pinto, P. A., Dhillon, V. S., Howell, & Harrop-Allin, M. K. 1997, MNRAS, 290, 663

Branch, D. 1999, ARAA, 36, 17

Calder A.C., Plewa T., Vladirova N., Brown E.F., Lamb D., Robinson K., Truran J.W. 2003, AAS 203, 4509C

Domínguez I., Höflich P. 2000, ApJ, 528, 854

Fesen R.A. 2005, in: Stellar Explosions in Multi-Dimensions, Cambridge University press, in press

Gamezo, V.N., Khokhlov, A.M. & Oran, E.S. 2004, Phys. Rev. Lett., 92, 211102

Gamezo, V.N., Khokhlov, A.M. & Oran, E.S. 2004, astro-ph/0409598.

Gamezo, V.N., Khokhlov, A.M., Oran, E.S., Chtchelkanova, A., Rosenberg, R.O. 2003, Science 299, 77

Höflich, P. & Stein, J. 2002, ApJ, 568, 779

Höflich, P., Gerardy, C., Linder, E., & Marion, H. 2003, Lecture Notes in Physics 635, Springer Press, p. 203 & astro-ph/0301334

Howell A., Höflich P., Wang L., Wheeler J. C. 2001, ApJ, 556, 302

Höflich, P., Khokhlov, A., Wheeler, J.C. 1995, ApJ, 444, 211

Höflich, P. 2005, Nucl. Phys. B, in press

Khokhlov A., Müller E., Höflich P. 1992, A&A, 253, L9

Khokhlov,A.,1995,ApJ,449,695

Khokhlov,A.,2001,astro-ph/0008463

Livne,E., Tuchman,Y. & Wheeler,J.C.,1992,ApJ,399,665

Livne,E.,1993,ApJ,412,634

Livne,E.,1993,ApJ,406,L17

Lisewski,A.M., Hillebrandt,W., Woosley,S.E., Niemeyer,J.C., Kerstein,A.R.,2000,ApJ,537,405L

Marietta,E., Burrows,A., & Fryxell,B.,2000,ApJ Suppl. 128, 615

Niemeyer,J.C. 1999,ApJ,523,57

Niemeyer,J.C., Hillebrandt,W. & Woosley,S.E.,1996, ApJ, 471,903

Niemeyer,J. & Hillebrandt,W.,1995,ApJ,452,779

Nomoto,K., Thielemann,F.K. & Yokoi,K. 1984,ApJ,286,644

Plewa,T., Calder,A.C & Lamb,D.Q. 2004, ApJ, 612,L37

Reinecke M., Hillebrandt W., Niemeyer J., Klein R., Gröbl A. 1999,A&A,347,724

Reinecke,M., Hillebrandt,W. & Niemeyer,J.C. 2002, A&A, 386,936

Reinecke,M., Hillebrandt,W. & Niemeyer,J.C. 2002,A&A, 391,1167

Röpke,F.K. & Hillebrandt,W. 2005,A&A, 431,635

Ruben,S. and Stephane,Z.,1999, Ann.Rev.of Fluid Mech.,31,567.

Wang, L., Baade,D., Höflich,P., Khokhlov,A., Wheeler,J.C., Kasen,D., Nugent,P., Perlmutter S., Fransson C., Lundqvist,P., 2003,ApJ,591,1110

Woosley,S.E., Wunch,S. & Kuhlen,M.,2004,ApJ,607,921

Wunch,S. & Woosley,S.E.,2004,ApJ, 616,1102

Yoon, S.-C. & Langer, N. 2004,A&A, 419, 623

Yoon, S.-C., Langer,N. & Scheithauer,S.,2004,A&A,425,217

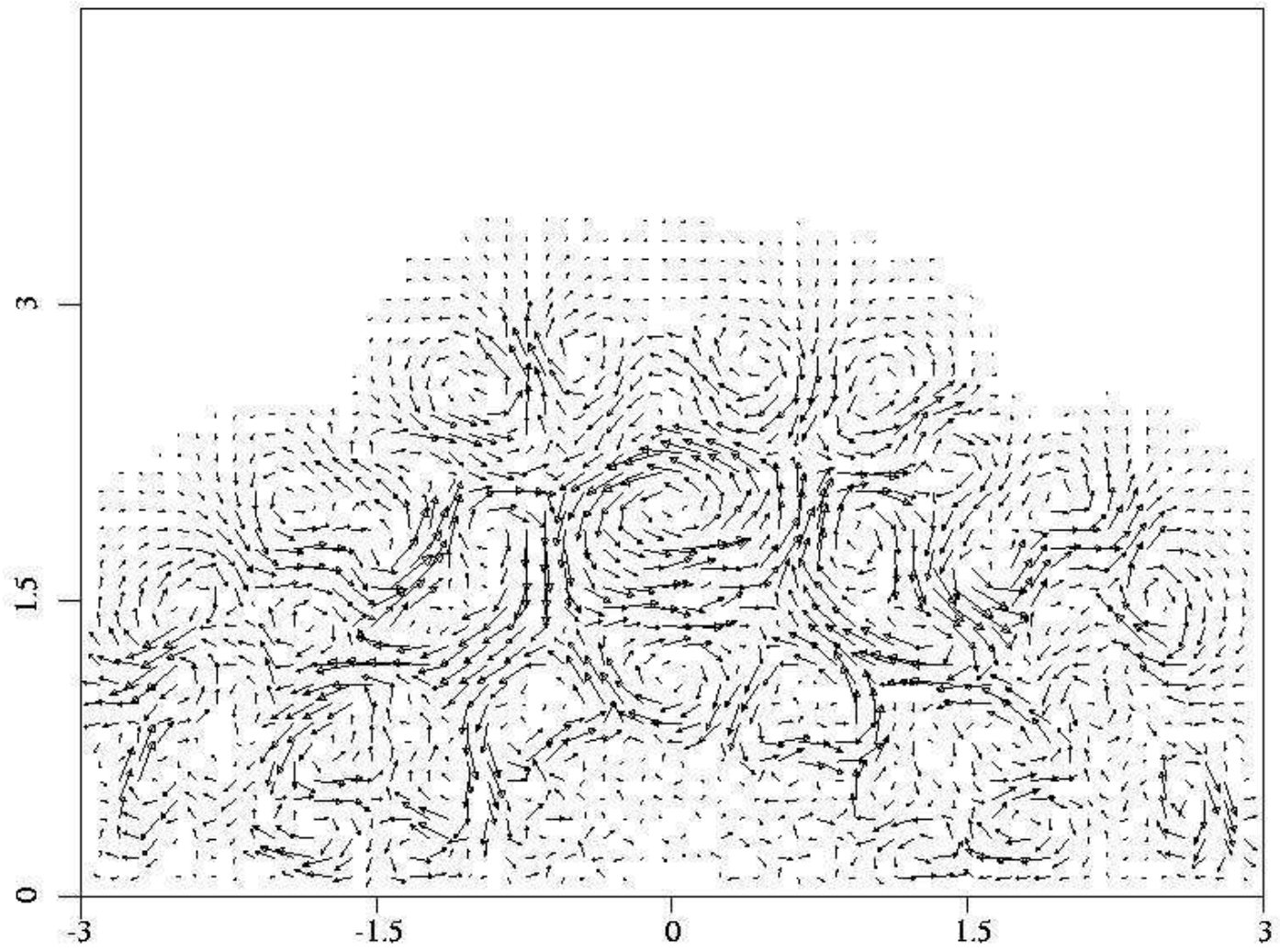
Fig. 1.— Initial convective velocity field. The longest arrows correspond to a velocity of 160 km/s. Only central region of star is presented. Unit scale on axes is 100 km.

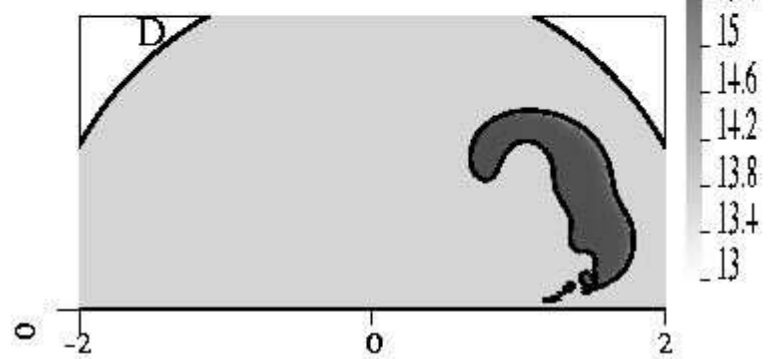
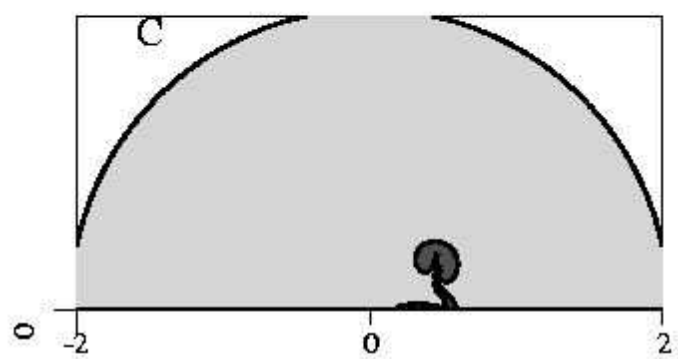
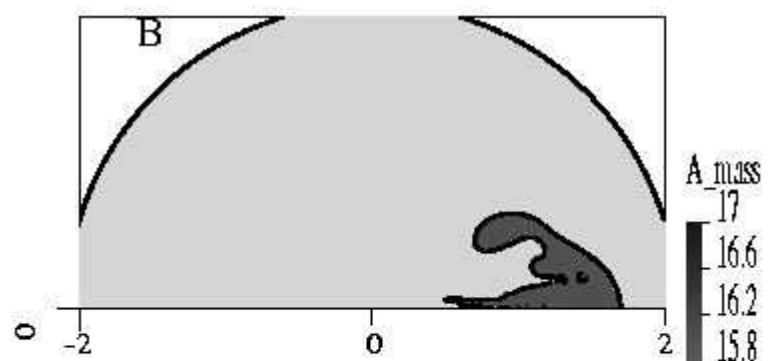
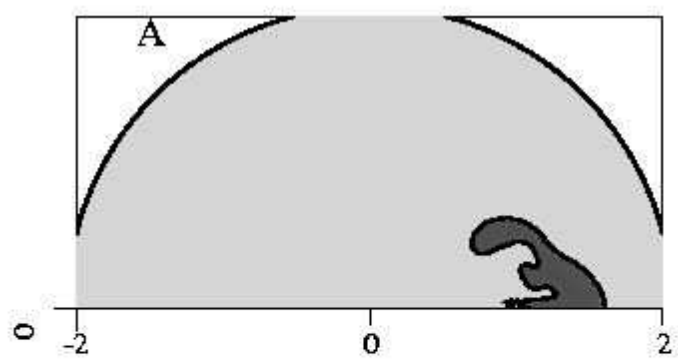
Fig. 2.— Burning region of simulations with single off-center ignition, at  $T=1.2$  s. Unit scale on axes is 1000 km. Four simulations are presented: A - Ignition at  $r=20$  km . B - Ignition at  $r=20$  km with initial convective velocity field. C - Ignition at  $r=10$  km . D - Ignition at  $r=100$  km .

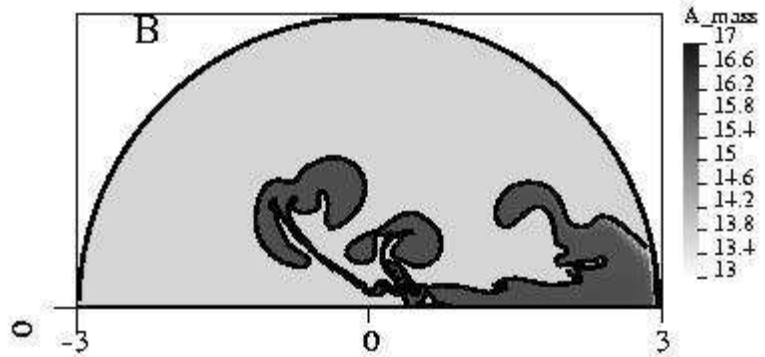
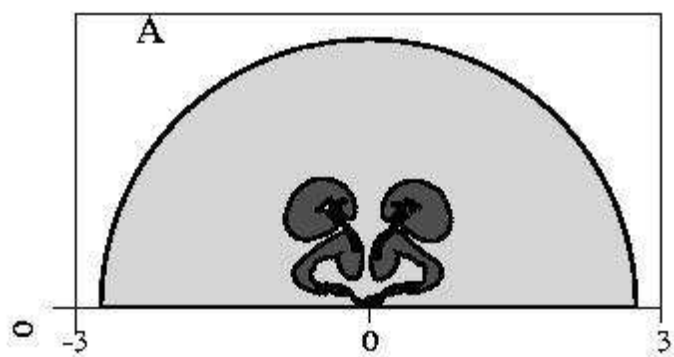
Fig. 3.— Burning region of simulations with central sphere ignition, at  $T=1.5$  s. Unit scale on axes is 1000 km. Two simulations are presented: A - no initial convective velocity field. B - with initial convective velocity field.

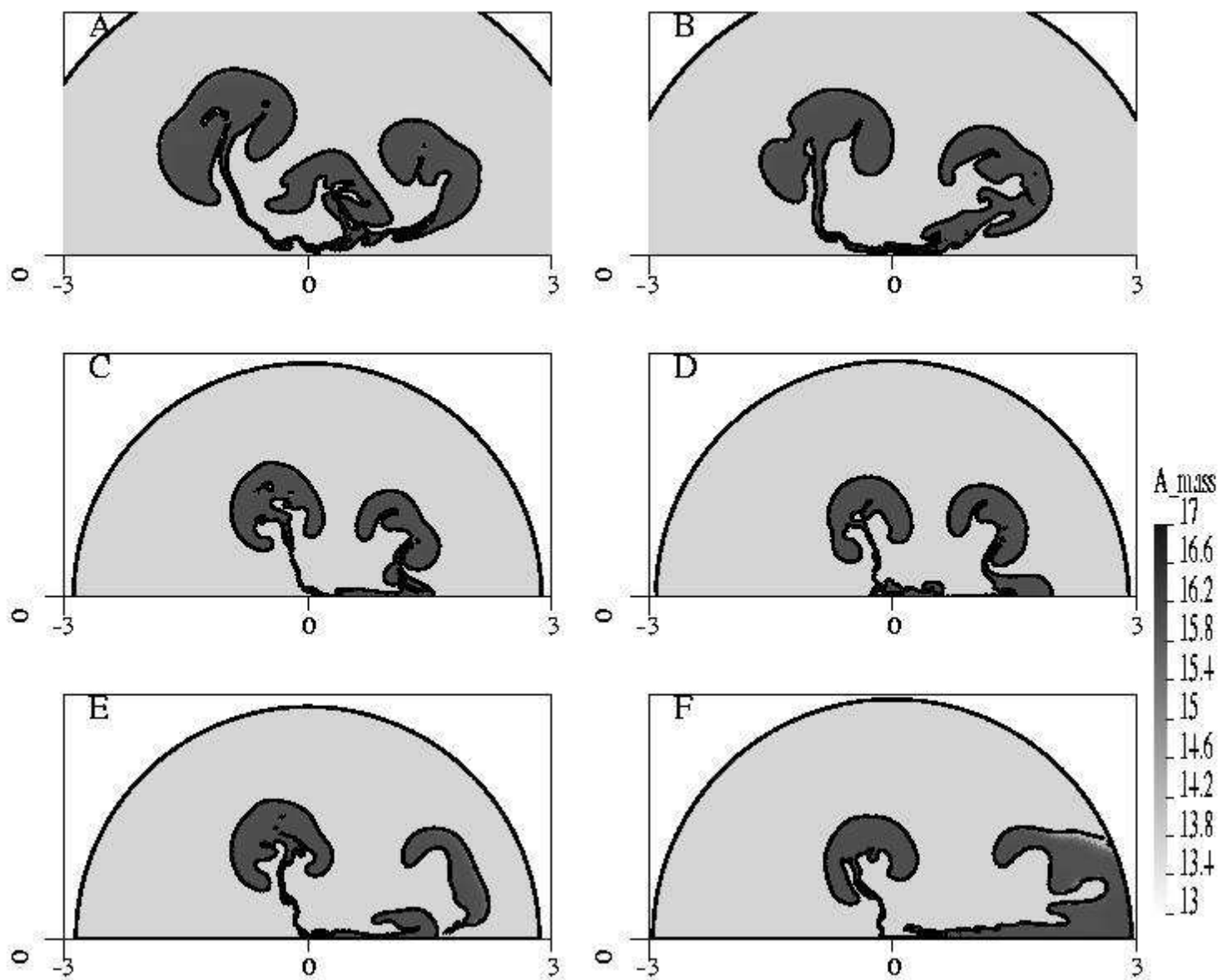
Fig. 4.— Burning region of simulations with multi-point ignition, at  $T=1.2$  s. Unit scale on axes is 1000 km. six simulations are presented: A - simultaneous ignition. B - simultaneous ignition with initial convective velocity field. C - non simultaneous ignition. D - non simultaneous ignition with initial convective velocity field. E - non simultaneous ignition, location of first ignition point on axis. F - non simultaneous ignition with initial convective velocity field, location of first ignition point on axis.

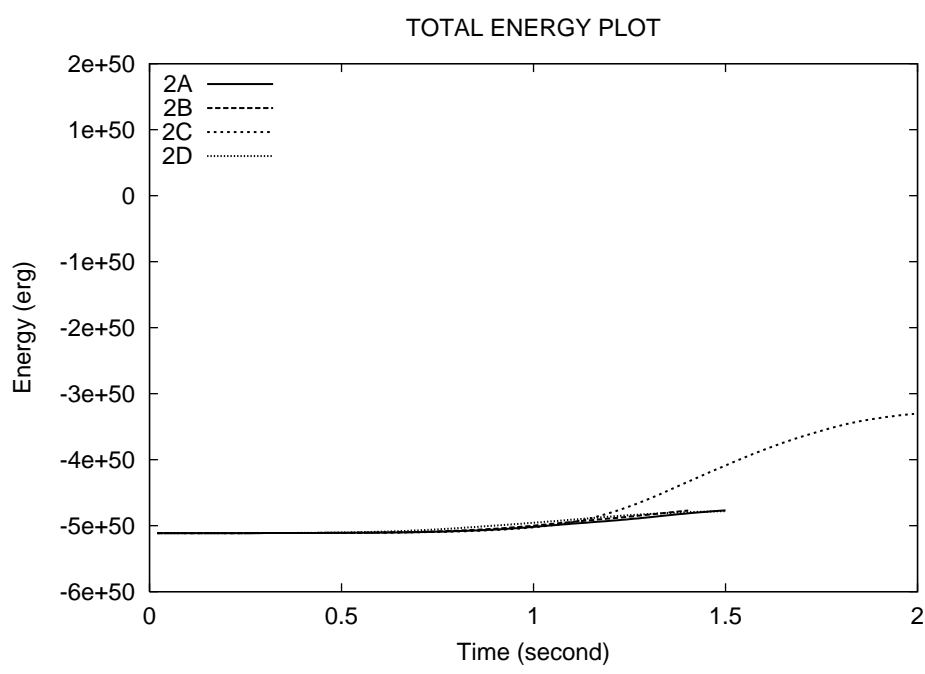
Fig. 5.— Total energy vs. time plot. Each simulation is marked by the figure number in which it's burning region is presented above. a - comparing single off-center ignition simulations. b - comparing central sphere ignition simulations. c - comparing multi-point ignition simulations. d - Energy production in the simultaneous multi-point simulation (fig. 4A) with three different resolutions.



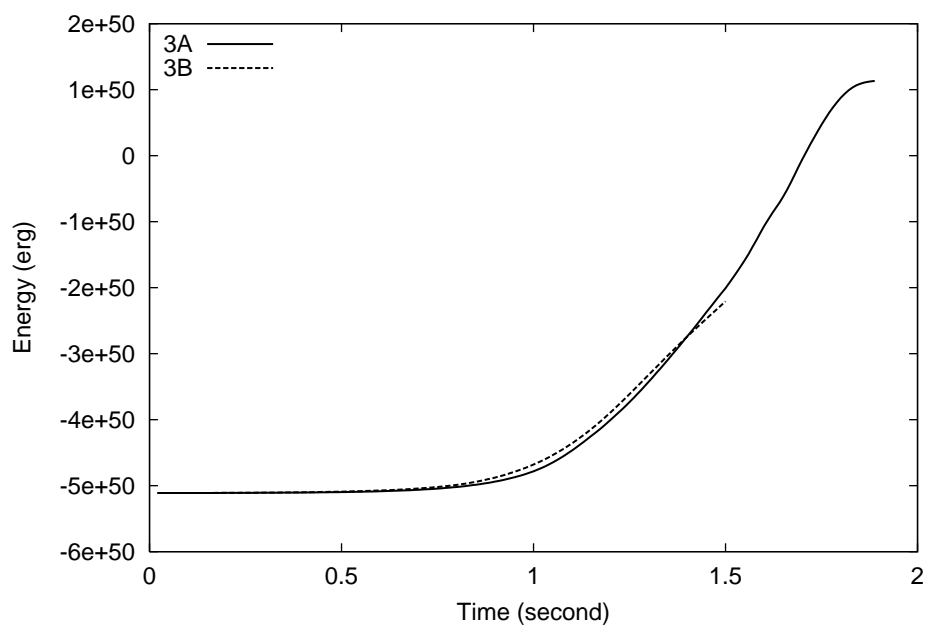


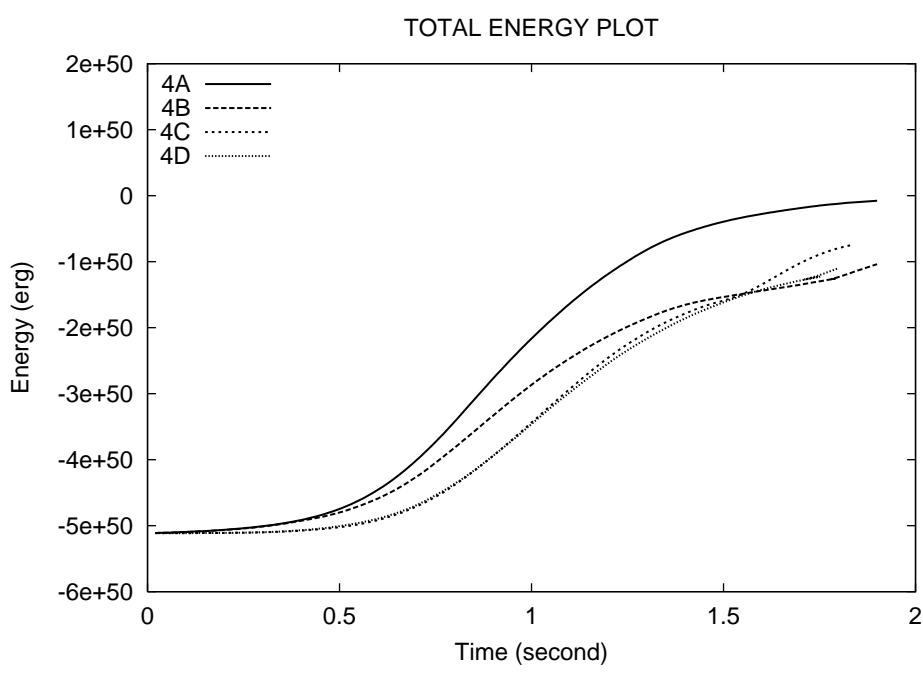






TOTAL ENERGY PLOT





TOTAL ENERGY PLOT

